Research Article

Journal of PeptideScience

Received: 9 December 2009 Revised: 27 April 2010 Accepted: 27 April 2010 Published online in Wiley Interscience: 25 June 2010

(www.interscience.com) DOI 10.1002/psc.1256

Syntheses and activities of backbone-side chain cyclic octapeptide ligands with *N*-functionalized phosphotyrosine for the *N*-terminal SH2-domain of the protein tyrosine phosphatase SHP-1

Mohammad Safa Zoda,[a] Martin Zacharias[b] and Siegmund Reissmann[a,‡*]

The protein tyrosine phosphatase SHP-1 plays an important role in many physiological and pathophysiological processes. This phosphatase is activated through binding of ligands to its SH2-domains, mainly to the N-terminal one. Based on a theoretical docking model, backbone-to-side chain cyclized octapeptides were designed as ligands. Assembly of such modelled structures required the synthesis of N-functionalized tyrosine derivatives and their incorporation into the sequence. Because of difficulties encountered in the condensation of N-protected amino acids to the *N*-alkylated tyrosine-peptide we synthesized and used preformed dipeptide building units. As all attempts to obtain phosphorylated dipeptide units failed, the syntheses had to be performed with a free phenolic function. Use of different *N*-alkyl or cycloalkyl residues in the N-functionalized side chains allowed to investigate the effect of ring size, flexibility and hydrophobicity of formed lactam bridges on stimulatory activity. All tested linear and cyclic octapeptides stimulate the phosphatase activity of SHP-1. Stimulatory activities of cyclic ligands increase with the chain length of the lactam bridges resulting in increased flexibility and better entropic preformation of the binding conformation. The strong activity of some cyclic octapeptides supports the modelled structure.

Supporting information may be found in the online version of this article

Keywords: backbone cyclization; dipeptide building blocks; stimulation of SHP-1; SH2-ligands; N-functionalized Tyr; phosphorylation; *O*-acylation; ligand modelling

Introduction

The cytosolic protein tyrosine phosphatase SHP-1 plays an important role in processing of immune cells, in cancer genesis and in cell adhesion and proliferation [2–10]. SHP-1 consists of 565 amino acids, assembled in 3 domains: N-terminal SH2-domain, C-terminal SH2-domain and the catalytic domain [11]. In the non-stimulated form the catalytic domain is shielded by the N-terminal SH2-domain. Activation by phosphotyrosine peptides takes place through binding to the SH2-domain, mainly to the N-terminal one. The evoked conformational changes liberate the catalytic domain resulting in enhanced phosphatase activity [11]. Substrates of SHP-1 are distinct phosphotyrosine residues in several kinases such as Ros- and Src-kinase [3,11–13], which are involved in cell signalling. Mainly such substrates are dephosphorylated, which are first phosphorylated by Src-kinase [13]. SHP-1 acts as negative regulator in the processing of allergic reactions [2,7–10], as a suppressor in the JAK/Stat-induced genesis of tumours [6], and protects nerve cells [14]. In Leishmanosis the elongation factor eF1α, expressed from trypanosomes, inactivates macrophages through stimulation of SHP-1 [15,16]. Through this activation of SHP-1 *leishmania* is able to survive in infected macrophages.

Some functionally important cellular proteins contain phosphotyrosine sequences, e.g. ITIM-sequences, to identify the N-terminal SH2-domain of SHP-1. Receptors of T- and B-cells, antigen receptors (CD22, 66, 72, and 84), the Epo-receptor, Ros-kinase, and Stat 5 belong to this family of proteins [17–19].

The purpose of this work was to develop octapeptides derived from the sequence of the receptor tyrosine kinase (RTK)-ROS, i.e. Leu-Asn-**p**Tyr-Met-Val-Leu [17,18,20], as activators of the

* *Correspondence to: Siegmund Reissmann, Institute of Biochemistry and Biophysics, Friedrich-Schiller-University Jena, Philosophenweg 12, D-07743 Jena, Germany. E-mail: siegmund.reissmann@uni-jena.de*

a *Institute of Biochemistry and Biophysics, Friedrich-Schiller-University Jena, Philosophenweg 12, D-07743 Jena, Germany*

b *Physik-Department (T38), Technische Universität München, James Franck-Str. 1, D-85748 Garching, Germany*

‡ *Preliminary accounts were published in Ref. [1].*

Abbreviations used: *Abu, α-amino butyric acid; γAbu, γ-amino butyric acid; δAva, δ-amino valeric acid; εAhc, ε-amino hexanoic acid; HOOC-C_6H_{10}-CH_2-NH_2, cis aminomethyl-cyclohexanoic acid; H_2N-CH_2-CH_2-C_6H_4-COOH, p-(aminoethyl) benzoicacid; Nle, norleucine; eq., equivalents; BTSA, N,O-bis(trimethylsilyl)acetamide; EtOH, ethanol; GST, glutathion S-transferase; MBHA, methoxybenzhydrylamine; MeCN, acetonitrile; MeOH, methanol; ITIM, immunoreceptor tyrosine-based inhibition motif; JAK, Janus kinase; PBS, Dulbecos PBS (phosphate buffer solution); PK, proteinase K; rt., room temperature; TFFH, tetramethylfluoroformamidinium hexafluorophosphate; TIS, triisopropylsilane.*

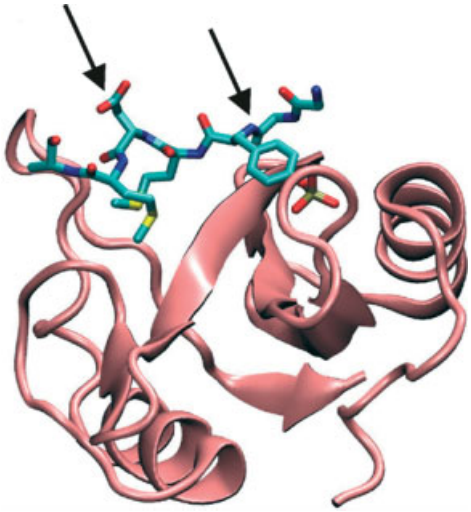

Figure 1. Modelled structure of ligands of the N-terminal SH2-domain with backbone-to-side chain cyclization. The crystal structure of the N-SH2-domain (pdb-entry:1AYC) is shown as cartoon (pink) and the bound phospho-peptide as stick model (atom colour coded, partial sequence pYMDM). The location of the backbone nitrogen of phosphotyrosine and the aspartic acid residue used as anchors for the backbone-to-side chain cyclization are indicated by arrows. The distance between the groups in the crystal structure is 9 Å.

protein tyrosine phosphatase SHP-1. Using a docking model [21,22] a basic structure was designed with N-functionalized phosphotyrosine for backbone-to-side chain cyclization. As these activating peptides would require a specific steric display of the phosphotyrosine side chain and backbone structure for high-affinity binding, the purpose of this study was to stabilize such spatial arrangement by a specific backbone-to-side chain cyclization bridge (Figure 1).

Furthermore, backbone cyclization was expected to stabilize these ligands against proteolytic degradation. Based on this concept peptides of the following general structure were synthesized:

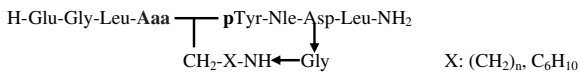

Assembly of such cyclic peptides requires synthesis and application of N-functionalized tyrosine derivatives. In the past decade, we have been involved in syntheses of N-functionalized amino acids [23–25] and of backbone cyclic analogues of the peptide hormones bradykinin [26,27] and somatostatin [27,28]. The synthesis of the cyclic phosphotyrosine peptides foresees backbone-to-side chain cylization starting at N-functionalized phosphotyrosine. However, until now backbone cyclization has been performed with bifunctional [23,24,28–34] and in a few cases with trifunctional [25] amino acids but never with phosphotyrosine.

To optimize the synthesis of these phosphotyrosine cyclic peptides, we studied the preparation of N-functionalized tyrosine derivatives, the coupling of the next amino acid to the *N*-alkylated tyrosine derivatives, and the assembly of the octapeptides. Preformed dipeptide building units were found to be essential for successful assembly of octapeptides with lactam bridges. This approach used tyrosine derivatives functionalized with different *N*-alkyl-, cycloalkyl- and aralkyl-groups to analyse the effect of the chemical properties of the lactam bridge on the biological activity of the SH2-ligands. Moreover, to reduce the synthetic difficulties Asn at position 4 was replaced by the isosteric Abu and Met at position 6 by Nle. The resulting enzymatic activities showed that octapeptides with Asn induce a stronger stimulatory activity than those with Abu. But, the reduction of activity by both replacements was found to be marginal and thus not to prevent the synthesis of analogues with moderate to high activity.

Materials and Methods

Materials

All chemicals, unless otherwise stated, were purchased from Fluka (Sigma-Aldrich Chemie, Seelze, Germany). Amino acid derivatives (Fmoc-Asn(Dmcp)-OH, H-Tyr(Bu^t)-OH, H-Tyr(Bu^t)-OBu^t) and coupling reagents were from Advanced ChemTec Europe (Bamberg, Germany) and Novabiochem (Bad Soden, Germany). TFFH was obtained from PE Biosystems (Weiterstadt, Germany), SASRIN-resin and Fmoc-Lys(Alloc)-OH) from BACHEM (Bubendorf, Switzerland), H-Abu-OH, H-βAla-OH, H-γAbu-OH, H-δAva-OH, H-εAhc-OH, *cis* aminomethyl-cyclohexyl-carbonic acid and H_2N-CH_2-CH_2-C_6H_4-COOH from Sigma-Aldrich Chemie (Taufkirchen, Germany), Hyacinth EMP from EMP-Biotech GmbH (Berlin, Germany), recombinant human SHP-1 from Enzo Life Sciences (Lörrach, Germany), PK (*Tritirachium album)* from Quiagen (Hilden, Germany), Dulbecos PBS (1×, without Ca and Mg) from 'The Cell Culture Company' (Pasching, Austria), Phosphatase Testkit and GST-tagged catalytic domain of SHP-1 from Jena Bioscience GmbH (Jena, Germany). All materials and solvents were of reagent grade and were used without further purification with the following exceptions: dimethylformamide (DMF) was first dried over molecular sieves and distilled from phthalic acid anhydride; dichloromethane (DCM) was stored over molecular sieves.

General Procedures

Thin-layer chromatography (TLC) was performed on precoated silica gel plates (silica gel 60 F_{254}, Merck, Darmstadt, Germany) with system 1 (S1) chloroform/methanol 9:1 (v/v), system 2 (S2) *n*-butanol/acetic acid/water 4/1/1 (v/v/v), system 3 (S3) benzene/acetone/acetic acid 27/10/0.5 (v/v/v), system 4 (S4) ethyl acetate/hexane 9/1 (v/v), system 5 (S5) *n*-butanol/acetic acid/water (8/3/4 v/v/v) and system 6 (S6) pyridine/ethyl acetate/acetic acid/water (5/5/1/1 v/v/v/v) as mobile phases. TLC detection was accomplished with UV-light, ninhydrine reagent and Cl_2/tolidine solution.

Flash-chromatography was performed with a 'Kieselgel 60' (0.040–0.063 mm, MERCK) layer in a glass frit of 10.4 cm diameter and a high of 6–7 cm.

Analytical high performance liquid chromatography (HPLC) was performed in system I on a Shimadzu LC-10AT chromatograph with a Vydac 218TP C5 column (4.6 × 250 mm) or in system II on JASCO chromatograph PU-987 also with Vydac 218TP C5 column. For elution 3 gradients were used; gradient 1: 00–80% B in 80 min, gradient 2: 20–80% B in 60 min, gradient 3: 10–70% B in 60 min. A was 0.1% trifluoroacetic acid (TFA) in water and B 0.1% TFA in acetonitrile. For all gradients the flow rate was 1.0 ml/min and detection was accomplished at 220 nm.

The crude linear and cyclic peptides were purified by semi-preparative HPLC on JASCO chromatograph PU-987 equipped with a Vydac 218 TP1010 column (100 × 10 mm, 300 Å, 5 µm

Journal of PeptideScience

particle size) using a gradient of 15–65% B in 120 min. Detection was accomplished at 220 nm. Mass spectrometry was performed with electrospray ionization mass spectrometry (ESI-MS) (TSQ-Quantum, Thermo Fischer (Dreieich, Germany).

For characterization of the dipeptide units by ^{1}H- and ^{13}C-NMR the probes were dissolved in DMSO-D_6. ^{1}H- and ^{13}C-NMR-spectra were recorded at 400 MHz (AVANCE 400 MHz, Brucker, Rheinstetten, Germany).

Synthesis of N-Protected Amino Aldehydes (General Procedure)

*Alloc-amino acids (**1, 4, 7, 10, 13, 16**)*

The synthesis was performed according to Loffet *et al* [35] and Guibe [36]. Briefly, the amino acids (25 mmol, 1.1 eq.) were dissolved in 30–50 ml aqueous Na_2CO_3 solution. After cooling to 0 °C, Alloc-Cl (1 eq.) was added in small portions over 2 h. The pH of the reaction mixture was maintained at >9. The reaction mixture was stirred at rt. for 30 h, washed with diethyl ether (3×), cooled again to 0 °C, slowly acidified with half-concentrated HCl to pH 1–2 and extracted with ethyl acetate (3×). The combined ethyl acetate extracts were washed (1 N HCl, NaCl-solution), dried and evaporated. The resulting oils (yield 80–90%) were analysed by HPLC and TLC (Table 1) and used without further purification.

*Dimethyl hydroxamates of Alloc-amino acids (Alloc-amino acid-DMHs) (**2, 5, 8, 11, 14, 17**)*

The syntheses were performed according to Nahm and Weinreb [37]. Briefly, to Alloc-amino acids (25 mmol, 1 eq.) and *N*,*O*-dimethylhydroxylamine hydrochloride (1 eq.) in 70 ml DCM *N*,*N*-diisopropylethylamine (DIPEA) (1.1 eq.) and dicyclohexylcarbodiimide (DCC) (1 eq.) were added at 0 °C. The solution was stirred for 1 h at 0 °C and left overnight at rt. The precipitate was filtered off, washed with ethyl acetate and the combined solvents were evaporated. The residue was dissolved in ethyl acetate and washed with aqueous 0.1 M $KHSO_4$ and sat. $NaHCO_3$. After drying with $MgSO_4$ the solvent was evaporated and the resulting oils (yield 80–90%) were analytically characterized by HPLC and TLC (Table 1) and used without further purification.

Table 1. *N*-Alloc-protected amino acids, their dimethyl hydroxamates and aldehydes

No.	Structure	TLC S1	S2	S3	S4
1	Alloc-NH-$(CH_2)_2$-COOH; Alloc-βAla-OH	0.35	0.5	0.25	
2	Alloc-NH-$(CH_2)_2$-CO-N(CH_3)-OCH_3		0.6	0.3	0.4
3	Alloc-NH$(CH_2)_2$-CHO		0.6	0.3	0.6
4	Alloc-NH-$(CH_2)_3$-COOH; Alloc-γAbu-OH	0.45	0.5		0.45
5	Alloc-NH-$(CH_2)_3$-CO-N(CH_3)-OCH_3		0.65		0.55
6	Alloc-NH-$(CH_2)_3$-CHO		0.65		0.65
7	Alloc-NH-$(CH_2)_4$-COOH; Alloc-δAva-OH	0.5	0.55		
8	Alloc-NH-$(CH_2)_4$-CO-N(CH_3)-OCH_3		0.7		0.5
9	Alloc-NH-$(CH_2)_4$-CHO		0.7		0.7
10	Alloc-NH-$(CH_2)_5$-COOH; Alloc-εAhc-OH	0.55	0.55		
11	Alloc-NH-$(CH_2)_5$-CO-N(CH_3)-OCH_3	0.9	0.75		
12	Alloc-NH-$(CH_2)_5$-CHO		0.75		0.75
13	Alloc-NH-CH_2-C_6H_{10}-COOH (*cis*)		0.65	0.35	0.4
14	Alloc-NH-CH_2-C_6H_{10}-CO-N(CH_3)-OCH_3		0.6	0.3	0.45
15	Alloc-NH-CH_2-C_6H_{10}-CHO		0.6		0.7
16	Alloc-NH-$(CH_2)_2$-C_6H_4-COOH		0.65	0.3	0.45
17	Alloc-NH-$(CH_2)_2$-C_6H_4-CO-N(CH_3)-OCH_3		0.65	0.35	0.4
18	Alloc-NH-$(CH_2)_2$-C_6H_4-CHO		0.65		0.75

*Alloc-amino aldehydes (**3, 6, 9, 12, 15, 18**)*

Alloc-amino aldehydes were prepared according to Fehrentz and Castro [38] and our own experience [23,25] and immediately used for reductive alkylation of tyrosine derivatives.

Briefly, the Alloc-amino acid-DMHs **2**, **5**, **8**, **11**, **14** or **17** (25 mmol, 1 eq.) were dissolved in 20 ml tetrahydrofuran (THF) (dried with Na and degassed with argon). After cooling to 0 °C, $LiAlH_4$ (1.2 eq.) was added in small portions to the cooled and stirred reaction mixture. Stirring was continued at rt. for 1 h and aqueous sat. $KHSO_4$ solution added. THF was removed *in vacuo* and the aqueous solution extracted (3×) with diethyl ether. After drying over Na_2SO_4, the ether was evaporated. The resulting oils (yield 80–90%) were chemically characterized (Table 1) and immediately used for reductive alkylation.

Synthesis of N-Functionalized Tyrosine Derivatives

*H-[$(CH_2)_3$-NH-Alloc]Tyr(Bu^t)-OH (**19**)*

H-Tyr(Bu^t)-OH (15 mmol, 1 eq.) was dissolved in dry MeOH containing 3 g molecular sieves and triethylamine (TEA) (1 eq.). Freshly prepared aldehyde **3** (1.1 eq.) was added to this solution. After stirring for 1 h at rt., the solution was cooled to 0 °C and $NaCNBH_3$ (1 eq.) was added in small portions over 30 min. Stirring was continued overnight at rt., the molecular sieve was removed and the solvent evaporated. The residue was dissolved in ethyl acetate and extracted with aqueous solutions of $KHSO_4$ and NaCl. After drying over Na_2SO_4, the ethyl acetate was evaporated and the resulting crude product was purified by flash-chromatography [ethyl acetate-hexane 0 : 10 (100 ml), 2 : 8 (200 ml), 4 : 6 (200 ml), 6 : 4 (200 ml), 9 : 1 (1000 ml), 10 : 0 (400 ml) v/v] and analytically characterized by HPLC, TLC, ESI-MS (Table 2) and H-, ^{13}C-NMR (Supporting Information) (yield: 10%).

*H-(X-NH-Alloc)Tyr(Bu^t)-OBu^t (**20, 21, 22, 23, 24, 25**) with X = $(CH_2)_3$, $(CH_2)_4$, $(CH_2)_5$, $(CH_2)_6$, CH_2-C_6H_{10}-CH_2, CH_2-C_6H_4-$(CH_2)_2$*

To H-Tyr(Bu^t)-OBu^t (25 mmol, 1 eq.) in dry MeOH (containing molecular sieves) and TEA (1 eq.) freshly prepared Alloc-amino aldehyde (**3, 6, 9, 12, 15** or **18**; 1.1 eq.) was added (Table 2). The reaction mixture was kept at rt. for 1 h and cooled to 0 °C; then $NaCNBH_3$ (1 eq.) was added in small portions over 30 min. After stirring overnight at rt., the molecular sieve was filtered off and the solvent evaporated. The residue was dissolved in ethyl acetate and extracted with aqueous solutions of $KHSO_4$ and NaCl. After drying over Na_2SO_4, the ethyl acetate was evaporated and the resulting crude product was purified by flash-chromatography (ethyl acetate–hexane 9 : 1 v/v) and analytically characterized by HPLC, TLC, ESI-MS (Table 2).

Synthesis of Protected Pseudo Dipeptide Building Units

*Fmoc-Abu-[$(CH_2)_3$-NH-Alloc)]Tyr(Bu^t)-OH (**26**)*

Compound **19** (1 mmol, 1 eq.) was suspended in 10 ml DCM, spiked with BTSA (3 eq.) and stirred for 24 h until a clear solution was obtained. Fmoc-Abu-F (2 eq.) was added in small portions to the stirred reaction mixture at 0 °C containing DIPEA (2 eq.).

Table 2. N-functionalized tyrosine derivatives

No.	Building Unit	HPLC t_R (min)	Yield (%)	TLC S_2	TLC S_3	Mol wt calculated	Mol wt found
	HNTyr(Bu^t)-OH					397.1	$[M+Na]^+$402.2
19	$(CH_2)_3$NHAlloc	16.5	10	0.31	0.35		$[M+K]^+$ 418.1
	HNTyr(Bu^t)-OBu^t					434.5	[M+H]$^+$ 435.7
20	$(CH_2)_3$NHAlloc	29.1	50	0.42	0.53		$[M+Na]^+$ 457.2
							$[M+K]^+$ 473.9
	HNTyr(Bu^t)-OBu^t					448.2	$[M+H]^+$ 449.5
21	$(CH_2)_4$NHAlloc	29.08	51	0.46	0.53		$[M+Na]^+$ 471.5
	HNTyr(Bu^t)-OBu^t					462.5	$[M+H]^+$ 463.8
22	$(CH_2)_5$NHAlloc	31.9	55	0.54	0.51		$[M+Na]^+$ 485.9
	HNTyr(Bu^t)-OBu^t					476.5	$[M+H]^+$ 477.2
23	$(CH_2)_6$NHAlloc	33.4	65	0.57	0.74		$[M+Na]^+$ 499.3
							$[M+K]^+$ 515.4
	HNTyr(Bu^t)-OBu^t					501.5	$[M+H]^+$ 502.2
24	CH_2-C_6H_{10}-CH_2NHAlloc	34.3	55	0.78	0.86		$[M+Na]^+$ 524.3
	HNTyr(Bu^t)-OBu^t					510.5	$[M+H]^+$ 511.4
25	CH_2-C_6H_4-$(CH_2)_2$NHAlloc	34.5	50	0.52	0.74		$[M+Na]^+$ 533.6

Yields are calculated from obtained amounts after purification by flash-chromatography.
HPLC was performed with system I, gradient 2.

Stirring was continued for 1 h at 0 °C, then the solvent was removed, the residue dissolved in 400 ml ethyl acetate, extracted with aqueous solutions of $KHSO_4$ and NaCl and dried over Na_2SO_4. The solvent was removed and the yellow oil was purified by flash-chromatography with ethyl acetate–hexane (4 : 6 400 ml, 7 : 3 600 ml, 9 : 1 1000 ml, 10 : 0 500 ml v/v) (yield: 9%). Analytical characterization was performed after cleavage of the *tert*-butyl ether. The product was identical to compound **33**.

*Fmoc-[$(CH_2)_3$-NH-Alloc]Tyr(Bu^t)-OH (**27**)*

Compound **19** (1 mmol) was treated in the same manner as described for the synthesis of **26**, except Fmoc-Abu-F was replaced by Fmoc-Cl (1.1 eq.). Yield: 85%.; HPLC: t_R = 44.1 min (system I, gradient 2); TLC: R_f (S1) = 0.6; M_r calcd.: 600.6; found 623.4, $[M+Na]^+$; 639.5, $[M+K]^+$; for ^{1}H- and ^{13}C-NMR see Supporting Information.

*Fmoc-Abu-[(X-NH-Alloc)]Tyr(Bu^t)-OBu^t (**28, 29, 30, 31, 32**); X = $(CH_2)_3$, $(CH_2)_4$, $(CH_2)_5$, $(CH_2)_6$, $CH_2-C_6H_{10}-CH_2$*

Fmoc-Abu-OH (4 mmol, 1 eq.), TFFH (1 eq.) and DIPEA (2 eq.) were dissolved in 10 ml DMF and allowed to react for 13 min; then H-(X-NH-Alloc)Tyr(Bu^t)-OBu^t (0.66 eq.) was added and the reaction mixture left for 4 h at rt. Coupling was repeated with 1 eq. of Fmoc-Abu-OH/TFFH/DIPEA (1 : 1 : 2). The solution was concentrated, diluted with 500 ml ethyl acetate, washed with aqueous $NaHCO_3$, NaCl, $KHSO_4$ and NaCl, dried and evaporated. The crude product was purified by flash-chromatography with an ethyl acetate/hexane gradient as for **26** and analytically characterized by HPLC, TLC and ESI-MS (Table 3).

Synthesis of Pseudo Dipeptide Units with Free Phenolic and Carboxyl Group (General Procedure)

*Fmoc-Abu-[(X-NH-Alloc)]Tyr-OH (**33, 34, 35, 36, 37**); X = $(CH_2)_3$, $(CH_2)_4$, $(CH_2)_5$, $(CH_2)_6$, $CH_2-C_6H_{10}-CH_2$*

The protected pseudo dipeptide building block Fmoc-Abu-(X-NH-Alloc)Tyr(Bu^t)-OBu^t was treated for 2 h with 50% TFA in DCM. The reaction mixture was then taken to dryness. The crude products were purified by flash-chromatography with an ethyl acetate/hexane gradient as described for **26** and chemically analysed by HPLC, TLC, ESI-MS (Table 4); for ^{1}H- and ^{13}C-NMR see Supporting Information.

*SASRIN-resin supported synthesis of Fmoc-Asn-[$(CH_2)_3$–NH-Alloc]Tyr-OH (**40**)*

[$(CH_2)_3$-NH-Alloc]Tyr(Bu^t)-*O*-SASRIN-resin (**38**): Fmoc-Tyr(Bu^t)-OH (1.5 eq.) was coupled to SASRIN-resin (loading 0.89 mmol/g) with *N,N′*-diisopropylcarbodiimide (DIC) (1.1 eq.) and 4-(dimethylamino)pyridine (DMAP) (0.01 eq.) in DMF/DCM (1 : 3 v/v) at 4 °C for 20 h. For capping of free amino groups the resin was reacted with benzoyl chloride (7 eq.) and pyridine (7 eq.) for 30 min. The loading was reduced to 0.6 mmol/g. After removal of the Fmoc-group and thorough washing, the resin was reacted with (Alloc-βAla-H (**3**) (2.5 eq.) and $NaCNBH_3$ in DMF containing 1% CH_3COOH.

Journal of PeptideScience

Table 3. Fully protected dipeptide building blocks

No.	Pseudodipeptides	t_R min.	Yield %	TLC S_3	TLC S_4	Mol wt calculated	Mol wt found
28	Fmoc-Abu(-$(CH_2)_3$NHAlloc)-Tyr(OBu^t)-OBu^t	55.5	70	0.65	0.8	741.4	$[M+H]^+$ 742.9 $[M+Na]^+$ 764.2
29	Fmoc-Abu(-$(CH_2)_4$NHAlloc)-Tyr(OBu^t)-OBu^t	56.4	70	0.65	0.8	755.4	$[M+H]^+$ 756.4 $[M+Na]^+$ 778.3 $[M+K]^+$ 794.2
30	Fmoc-Abu(-$(CH_2)_5$NHAlloc)-Tyr(OBu^t)-OBu^t	57.7	90	0.72	0.81	769.4	$[M+H]^+$ 770.5 $[M+Na]^+$ 792.8
31	Fmoc-Abu(-$(CH_2)_6$NHAlloc)-Tyr(OBu^t)-OBu^t	59.1	90	0.75	0.85	783.3	$[M+H]^+$ 784.9 $[M+K]^+$ 822.6
32	Fmoc-Abu(-CH_2-C_6H_{10}-CH_2-NHAlloc)-Tyr(OBu^t)-OBu^t	59.4	80	0.75	0.9	808.3	$[M+H]^+$ 809.2 $[M+Na]^+$ 831.6 $[M+K]^+$ 847.4

Yield after purification by flash-chromatography; HPLC: system I, gradient 2.

Table 4. Dipeptide building blocks with free phenolic and carboxyl group

No.	Pseudodipeptides	Yield %	t_R min.	TLC S_1	TLC S_3	F.	Mol wt calculated	Mol wt found
33	Fmoc-Abu(-$(CH_2)_3$NHAlloc)-Tyr-OH	50	32.7	0.45	0.40	110-113	629.4	$[M+H]^+$ 630.2 $[M+Na]^+$ 652.3 $[M+K]^+$ 669.1
34	Fmoc-Abu(-$(CH_2)_4$NHAlloc)-Tyr-OH	50	34.3	0.45	0.45	107-110	643.4	$[M+H]^+$ 644.1 $[M+Na]^+$ 666.2 $[M+K]^+$ 682.1
35	Fmoc-Abu(-$(CH_2)_5$NHAlloc)-Tyr-OH	90	35.5	0.55	0.45	101-104	657.4	$[M+H]^+$ 658.1 $[M+Na]^+$ 680.3 $[M+K]^+$ 696.2
36	Fmoc-Abu(-$(CH_2)_6$NHAlloc)-Tyr-OH	90	35.7	0.55	0.5	125-127	671.3	$[M+H]^+$ 672.1 $[M+Na]^+$ 694.3 $[M+K]^+$ 710.2
37	Fmoc-Abu(-CH_2-C_6H_{10}-NH-Alloc)-Tyr-OH	75	37.7	0.6	0.55	117-121	696.5	$[M+H]^+$ 697.1 $[M+Na]^+$ 720.3 $[M+K]^+$ 736.2
40	Fmoc-Asn(-$(CH_2)_3$NHAlloc)-Tyr-OH	50	26.4	0.35	0.3	173-175	658.4	$[M+H]^+$ 659.5 $[M+Na]^+$ 681.2 $[M+K]^+$ 697.2

Yield after purification by flash-chromatography; HPLC: system I, gradient 2.

Fmoc-Asn(Dmcp)-[$(CH_2)_3$-NH-Alloc]Tyr(Bu^t)-*O*-SASRIN-resin (**39**): Fmoc-Asn(Dmcp)-OH (4 eq.) was coupled to resin-bound functionalized tyrosine **38** with hexafluorophosphate (HATU) (4 eq.), HOAt (4 eq.) and DIPEA (8 eq.) over 4 h; yield: 65%; HPLC (after removal of protected peptide from SASRIN-resin): t_R = 47.9 min (system I, gradient 2).

Fmoc-Asn-[$(CH_2)_3$-NH-Alloc]Tyr-OH (**40**): After removal from the resin with 1% TFA in DCM and evaporation of the solvent the residue was treated with 50% TFA in DCM for 2 h. The concentrated solution was diluted with 200 ml ethyl acetate and extracted with aqueous solutions of $KHSO_4$ and NaCl. After drying over Na_2SO_4, the solution was taken to dryness; yield: 60%. The crude product was purified by flash-chromatography and chemically analysed by HPLC, TLC, F., ESI-MS (Table 4); for ^{1}H- and ^{13}C-NMR see Supporting Information.

Assembly of Linear Peptides

The linear octapeptides were synthesized by the solid phase method on Rink-amide-MBHA resin. The C-terminal Leu was attached to the resin (loading 0.73 mmol/g) as pentafluorophenyl ester. Only 1 eq. of Fmoc-Leu-OPfp was used to reduce loading of the resin, followed by capping with Z(2-Cl)-OSu. Coupling of the building unit Fmoc-Asp(Gly-OAll)-OH [39] (3 eq.) was performed using TFFH. For coupling of Fmoc-Nle-OH (4 eq.) a

mixture was used of 4 eq. PyBOP, 4 eq. HOBt and 6 eq. DIPEA in DMF. The preformed dipeptide building blocks (3 eq. each, **33–37, 40**) were coupled using 3 eq. PyBOP, 3 eq. HOBt and 6 eq. DIPEA. Fmoc-Leu-OPfp (4 eq.) and Fmoc-Gly-OPfp (4 eq.) were used for the next two coupling steps. Coupling of the N-terminal Glu was carried out with Boc-Glu(OBu^t)-OH (4 eq.) using PyBOP/HOBt/DIPEA (4 eq.). Each coupling was repeated twice with a coupling time of 60 min each. Only for the dipeptide units the reaction time was prolonged to 180 min. Each step was checked by HPLC, ESI-MS and evaluated by the UV-spectrophotometric determination of Fmoc-piperidine adduct. Removal of Fmoc-group was performed with 20% piperidine in DMF in 2 steps (5 and 10 min).

Cyclization on Solid Support

Removal of Alloc- and allyl-ester protection was carried out using the conventional method with $Pd^0(PPh_3)_4$ in DMF/THF/HCl 0.5 N/morpholine = 2 : 2 : 1 : 0.9 under argon overnight [40]. The cyclization was performed twice using 5 eq. PyBOP/HOBt as coupling reagent and 10 eq. diisopropylethyl amine (DIEA) as a base, 3 h for each. The cyclization process was monitored by analytical HPLC.

Phosphorylation of octapeptides on solid support [41–43]

For phosphorylation the resin-bound cyclic octapeptides were thoroughly dried (using P_2O_5) and allowed to react with di-*tert*-butyl diisopropyl phosphoamidite (20 eq.) and the catalyst Hyacynth BMT (60 eq.) in a small volume of DMF/DCM for 1 h. To complete the phosphorylation this reaction was repeated twice or more. Oxidation was carried out with *tert*-butyl-hydroperoxide or *m*-Cl-peroxybenzoic acid in DCM. After thoroughly washing with DCM the resin-bound peptides were dried.

Deprotection and Resin Cleavage of the Octapeptides Derivatives

The linear and cyclic peptides were obtained by resin cleavage and deprotection of the Boc-, Trt- and $P(OBu^t)_2$-groups with 95% TFA, 2.5% TIS and 2.5% H_2O for 6 h. Yields of crude products calculated from resin loading with linear precursor: 20%.

Purification and Characterization of the Octapeptide Derivatives

After concentrating the TFA-cocktail to 1 ml, followed by precipitation with ether and separation by centrifugation, the pellets were thoroughly washed with ether, dissolved in aqueous *tert*-butanol (80%) and the solutions were filtered through glass wool, lyophilized and purified by semi-preparative HPLC as described under general methods. The compounds were homogeneous on HPLC and showed the expected masses in ESI-MS (Table 5).

Stability Against Proteolytic Degradation

The octapeptides **OP 2** and **OP 8** (150 µg each) were dissolved in 150 µl buffer (PBS, pH 7.0–7.5). Proteolytic cleavage was started at 0 °C by addition of 142 µl buffer and 8 µl PK (8 DMC-U/ml). Proteolytic cleavage was monitored at rt. Aliquots were taken after 2, 20, 60 and 120 min and analysed by HPLC in system II with gradient 2.

Stimulation of Protein Tyrosine Phosphatase SHP-1 by the Octapeptide Ligands

The phosphatase assay was performed with a Test-Kit from Jena Bioscience GmbH in a 96-well plate according to the instructions. The substrate *p*-nitrophenylphosphate was used in a concentration of 10 mM, the enzyme SHP-1 at concentrations of 15 and 30 nM. The linear and cyclic octapeptides, phosphorylated or non-phosphorylated, were applied in increasing concentrations from 25 to 500 µM. After 1 h at pH 8.5 the reaction was stopped with 1 N NaOH and the amount of formed *p*-nitrophenol was estimated by a plate reader ('Fluostar/Polarstar Galaxy', BMG Labtechnologies). In addition to the stimulatory activity, computer-aided calculations provide a quotient between found stimulation and basal activity of the actually used amount or preparation of the enzyme. The measurements were carried out in a triplicate and the results are given as the average of two independent experiments. The values were in the range of ±15%.

Results and Discussion

Dipeptide Building Blocks

For the synthesis of the planned set of modelled octapeptide ligands a series of N-functionalized tyrosine derivatives were used. To study the influence of direction, flexibility and hydrophobicity of the lactam bridge between backbone and side chain, tyrosine derivatives with corresponding properties in the functionalized side chain were prepared. Using our experience in this field [23–28], we started with the synthesis of corresponding aldehydes. The N-protected amino aldehydes (**3, 6, 9, 12, 15, 18**) were obtained through Alloc-protected amino acids (**1, 4, 7, 10, 13, 16**) and their dimethyl hydroxamates (**2, 5, 8, 11, 14, 17**) (Table 1), characterized by TLC and immediately used for reductive alkylation of tyrosine derivatives.

The tyrosine derivatives H-Tyr(Bu^t)-OH and H-Tyr(Bu^t)-OBu^t, respectively, were used for reductive alkylation with *N*-Alloc-protected amino aldehydes yielding the N-functionalized tyrosine derivatives **19–25**. The resulting compounds **20–25** are listed in Table 2. Although compounds **1–18** were used as crude products, the building blocks **19–25** were purified by flash-chromatography and analytically well characterized.

As coupling of Fmoc-protected amino acids to the polymer bound *N*-alkylated tyrosyl-peptide occurs to low extents (<50%), despite different attempts by changing coupling reagents, preformed dipeptide building blocks with tyrosine were used for the assembly of backbone-to-side chain cyclic peptides (Scheme 1).

All our different attempts to synthesize in solution or on SASRIN-resin the dipeptide building units with phosphorylated tyrosine failed. Indeed, we were unable to couple N-protected amino acids in more than 10% yield to an *N*-alkylated phosphotyrosyl-peptide. Thus, phosphorylation of resin-bound peptides had to be performed after assembly of pentapeptides or octapeptides. We preferred to phosphorylate the protected resin-bound octapeptides after cyclization. By this approach simultaneously both the phosphorylated and unphosporylated tyrosine-peptides became advantageously accessible.

Consequently, the synthesis had to be performed with dipeptide building units with an unprotected tyrosine residue, despite the expected side reactions at the free phenolic group. As coupling of Fmoc-Abu-OH to the N-functionalized tyrosine derivative with

Journal of PeptideScience

Table 5. Chemical characterization of the cyclic octapeptides

Peptide	Sequence	t_R min	TLC S_5	TLC S_6	Mol wt calcd.	Mol wt found
OP 4	H-Glu-Gly-Leu-Asn(-$(CH_2)_3$-NH-) **p**Tyr-Nle-Asp-Leu-NH_2 (Asn-Gly)	24.9*	0.6	0.7	1110.2	$[M+H]^+$ 1111.8 $[M+Na]^+$ 1132.8
OP 5	H-Glu-Gly-Leu-Abu(-$(CH_2)_3$-NH-) **p**Tyr-Nle-Asp-Leu-NH_2 (Abu-Gly)	26.2*	0.65	0.75	1082.2	$[M+H]^+$ 1083.3 $[M+Na]^+$ 1105.3 $[M+2H]^{++}$ 542.3 $[M+2Na]^{++}$ 462.3
OP 6	H-Glu-Gly-Leu-Abu(-$(CH_2)_3$-NH-) Tyr-Nle-Asp-Leu-NH_2 (Abu-Gly)	29.1*	0.65	0.75	1002.4	$[M+H]^+$ 1003.5 $[M+Na]^+$ 1025.4 $[M+2Na]^{++}$ 524.1
OP 7	H-Glu-Gly-Leu-Abu(-$(CH_2)_4$-NH-) **p**Tyr-Nle-Asp-Leu-NH_2 (Abu-Gly)	20.0** 21.2**	0.45	0.4	1095.5	$[M+H]^+$ 1096.4 $[M+Na]^+$ 1118.6 $[M+2H]^{++}$ 548.6 $[M+2Na]^{++}$ 571.0
OP 8	H-Glu-Gly-Leu-Abu(-$(CH_2)_5$-NH-) **p**Tyr-Nle-Asp-Leu-NH_2 (Abu-Gly)	21.3** 21.9**	0.45	0.35	1109.4	$[M+H]^+$ 1110.6 $[M+Na]^+$ 1132.5 $[M+2Na]^{++}$ 577.7
OP 9	H-Glu-Gly-Leu-Abu(-$(CH_2)_6$-NH-) **p**Tyr-Nle-Asp-Leu-NH_2 (Abu-Gly)	24.9**	0.45	0.45	1123.2	$[M+H]^+$ 1124.4 $[M+Na]^+$ 1146.5
OP 10	H-Glu-Gly-Leu-Abu(-CH_2-C_6H_{10}-CH_2-NH-) **p**Tyr-Nle-Asp-Leu-NH_2 (Abu-Gly)	22.7**	0.5	0.4	1149.5	$[M+H]^+$ 1150.4 $[M+Na]^+$ 1172.6 $[M+2Na]^{++}$ 597.8

HPLC: * system I, gradient 2; ** system II, gradient 2. Double peaks indicate partial racemization during coupling of dipeptide units.

free carboxyl group, i.e. H-[$(CH_2)_3$-NH-Alloc]Tyr(Bu^t)-OH (**19**) led to poor yields, the fully protected N-functionalized tyrosine derivatives were used for the synthesis of the target dipeptide units. Indeed, acylations of H-(X-NH-Alloc)Tyr(Bu^t)-OBu^t (**20–25**) produced the purified compounds **28–32** in 50–90% yield. In one case, by coupling Fmoc-Abu-OH to compound **25** with an aromatic residue in the functionalized side chain, the crude product could not be purified. Fmoc-Abu-OH, by-products and dipeptide unit were coeluted in flash-chromatography, even changing eluent gradients. In contrast to Fmoc-Abu-OH, all applied Fmoc-Asn-OH derivatives [Asn, Asn(Trt), Asn(Dmcp)] reacted with the fully protected tyrosine derivative only to a very low extent (Table 4). Even the use of microwave technique (80 Watt) [44] and enhanced temperatures [45] provided completely unacceptable yields. To overcome the low coupling rates we synthesized these dipeptide building units on SASRIN-resin, which allows the application of a higher excess of Asn-derivatives and repeated couplings. Thereby a dipeptide derivative was formed with a yield of 50% (estimated by analytical HPLC), which was sufficient for further purification.

All synthesized dipeptide derivatives were purified twice by flash-chromatography, once in the fully protected form (Table 3) and then after removal of both *tert*-butyl groups (Table 4). The analytically well-characterized dipeptides with free phenolic and carboxyl group were stored as stable powders.

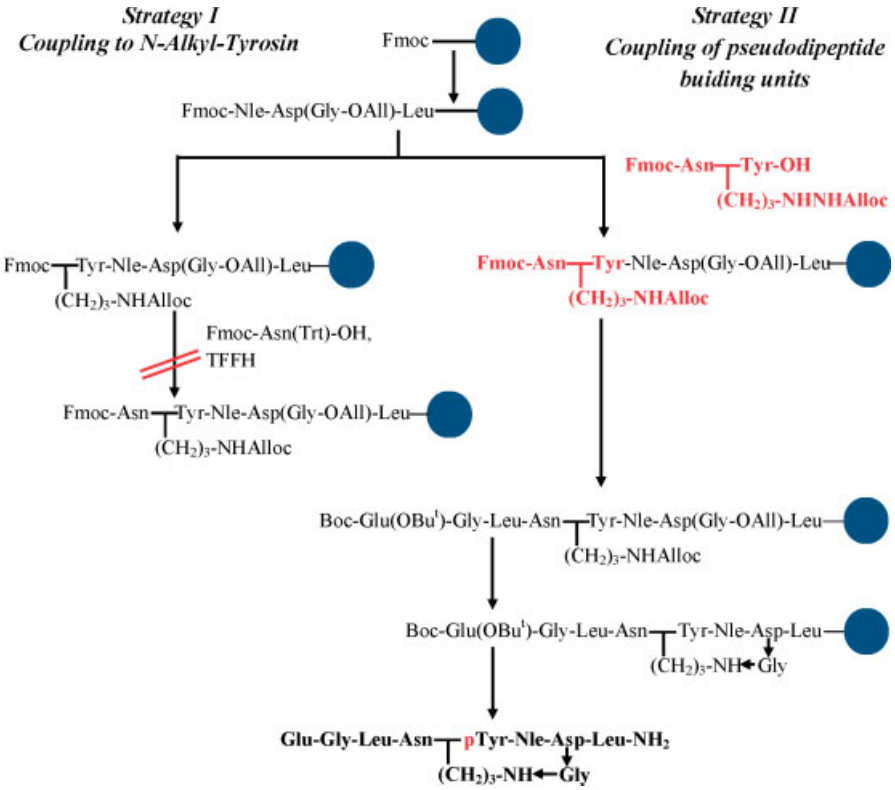

Scheme 1. Different strategies for assembly of the backbone-to-side chain cyclic octapeptides.

We were not able to synthesize N-functionalized tyrosine derivatives containing carboxyalkyl side chains. The reductive alkylation of H-Tyr(Bu^t)-OBu^t did not provide sufficient yields or purity of the desired compounds using either AllOOC-CH_2-COH or AllOOC-CH_2-CH_2-COH. Therefore we were unable to form lactam bridges with different amide bond direction. Furthermore, all attempts to synthesize dipeptide building blocks of the general formula Fmoc-AaaΨ[CH_2-N(CO-$(CH_2)_n$-NH-Alloc)]Tyr(Bu^t)-OX (with X = Bu^t, SASRIN-resin), containing an acylated reduced peptide bond between Aaa and Tyr failed. In this case we were unable to couple the activated Alloc-protected amino acids **1** and **4** in solution to the pseudodipeptide Fmoc-AsnΨ(CH_2-NH)Tyr(Bu^t)-OBu^t and on solid support to Fmoc-Asn(Dmcp)Ψ(CH_2-NH)Tyr(Bu^t)-*O*-SASRIN. In these acylation reactions activation of **1** and **4** with TFFH, DIC with HOAt, PyBrop as well as formation of fluorides, chlorides and mixed anhydrides were attempted.

Assembly of the Octapeptide Derivatives: Synthetic Strategies and Chemical Characterization

The strategy used for the synthesis of the cyclic octapeptide derivatives was shown in Scheme 1. The purified *N*-alkylated dipeptide building blocks with free carboxyl and phenolic groups (**33, 34, 35, 36, 37, 40**) were coupled to the resin-bound tripeptide under the same conditions as Fmoc-protected amino acids. Thus, activation of these dipeptide derivatives was performed with PyBOP. In contrast to urethane-protected amino acids, the preformed dipeptide derivatives can racemize to some degree during activation. In particular, higher base concentrations and longer coupling times can lead to partial racemization. Therefore, these coupling steps had to be thoroughly monitored. Nevertheless, the two octapeptides **OP 7** and **OP 8** showed two peaks in the analytical HPLC with the identical mass (Table 5).

Condensation of Fmoc-amino acids to the growing peptide chain with unprotected phenolic group was carried out with pentafluorophenyl esters, but in an intermediate step an Fmoc-aminoacyl-phenyl ester was formed. By treatment with piperidine for removal of the Fmoc-group this ester is simultaneously cleaved. This type of side reaction was first described by Paul [46] and later investigated by Svachkin *et al*. [47] and Martinez *et al*. [48]. We detected such ester formation by analytical characterization of the intermediates by HPLC coupled with ESI-MS.

After finishing the assembly, the resulting polymer bound octapeptides were consecutively cyclized, phosphorylated, cleaved from the resin and purified by HPLC. Cyclization and phosphorylation reactions were monitored by analytical HPLC and staining reactions and when required repeated to achieve completeness. Phosphorylation of resin-bound octapeptides with free phenolic group was performed with a concentrated reaction mixture [41]. Application of preformed dipeptide building blocks enabled us to obtain the target octapeptide compounds in satisfactory yields and at a high degree of homogeneity.

Stability Against Proteolytic Degradation

With the aim to check the stability against proteolytic degradation, the linear and cyclic peptides were incubated with PK as well as with a cell homogenates. PK is a highly active and very unspecific serine protease, isolated from mushrooms. This enzyme acts as exo- and endoprotease and is applied in food monitoring for differentiation between native and misfolded prions. Figure 2 shows that the high activity of PK completely degrades the linear octapeptide **OP 2** in less than 20 min, whereas the cyclic peptide **OP 8** remains stable over a period of 120 min. The cyclic octapeptide was also stable (not shown) with a cell homogenate (NIH 3T3).

Journal of PeptideScience

Biological Activities

The phosphatase SHP-1 requires stimulation by ligands for their SH2-domains. In the non-stimulated state the N-terminal SH2-domain binds to the catalytic domain and blocks the phosphatase activity [11], whereas ligands of the N-terminal SH2-domain can open this self-inhibiting structure. Pei and colleagues [20] concluded from results using large peptide libraries that stimulation of phosphatase activity of SHP-1 is directly correlated with the binding affinity of a ligand to the N-terminal SH2-domain. Table 6 shows the stimulation of a recombinant human SHP-1 by the octapeptide ligands. To avoid interactions with affinity tags commonly used for purification [20], free SHP-1 was used. All tested octapeptide ligands stimulated the phosphatase activity. Ligands with strong stimulatory activities showed estimated EC_{50} values in the low micromolar range (<10 μM). The stimulatory activity decreased only at higher concentrations, and not below the basal value. None of our octapeptides reduced the basal activity of the SHP-1. The octapeptides **OP 2 and OP 8** showed only marginal influence on the activity of the GST-tagged catalytic domain at higher concentrations (250–500 μM), indicating that they do not act as phosphatase inhibitors.

The stimulatory activities allow for the following conclusions: The phosphorylated octapeptides (**OP 1** and **OP 2**) stimulate better than the non-phosphorylated **OP 3**. In these octapeptide sequences the phosphate group contributes by about 60% to the binding affinity to a SH2-domain. But the contribution of the phosphate group depends on the type of SH2-domain and on ligand sequence and activity. Generally, the SH2-domain can bind to non-phosphorylated peptides and nonpeptide ligands as well as to compounds with phosphotyrosyl mimetics.

The residue Asn at position 4 (**OP 1, OP 4**) leads to a slightly higher affinity for the SH2-domain than Abu at this position (**OP 2, OP 5**). This finding agrees well with the results reported by Pei *et al*. [18,20]. The bound peptides require a specific steric display of the side chain and backbone structure for high-affinity binding. The aim of this study was to stabilize such spatial arrangement by a backbone-to-side chain cyclization bridge. The results indicate that even the smaller linkers are in principle sufficient to bridge the distance of approximately 9 Å between the anchor groups on the peptide as determined in modelling experiments. The steric bulkiness of the linker may interfere with the formation of the bound peptide structure and consequently lower the activation effect. With larger side chain linkers the access to the specific backbone structure required for higher affinity binding

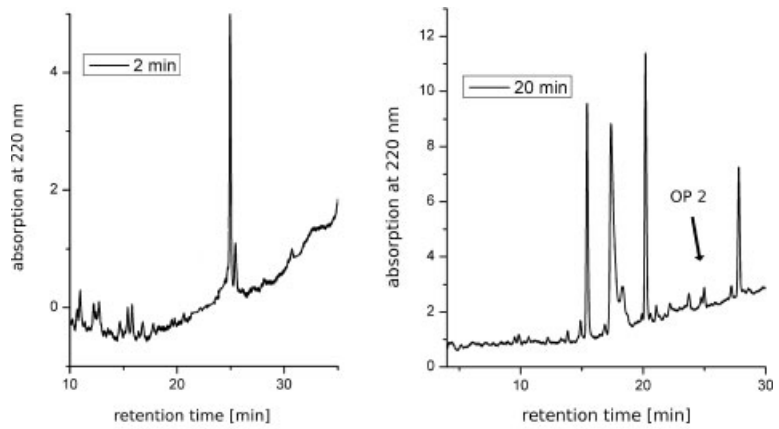

Figure 2. Lability of linear octapeptide **OP 2** and stability of cyclic octapeptide **OP 8** against PK. **OP 2** and **OP 8** were incubated with PK and the proteolytic cleavage was analysed by HPLC. First aliquots (0–2 min) were taken from the complete incubation medium at about 0 °C.

Table 6. Stimulation of phosphatase activity of SHP-1 by linear and cyclic octapeptides

Peptide	Structure	Activity	Ring size
	Basal activity of SHP-1	1	
OP 1	H-Glu-Gly-Leu-Asn-**p**Tyr-Nle-Asp-Leu-NH_2	9.5	0
OP 2	H-Glu-Gly-Leu-Abu-**p**Tyr-Nle-Asp-Leu-NH_2	7.5	0
OP 3	H-Glu-Gly-Leu-Abu-Tyr-Nle-Asp-Leu-NH_2	4.5	0
OP 4	H-Glu-Gly-Leu-Asn-**p**Tyr-Nle-Asp-Leu-NH_2 $(CH_2)_3$-NH ← Gly	5.0	17
OP 5	H-Glu-Gly-Leu-Abu-**p**Tyr-Nle-Asp-Leu-NH_2 $(CH_2)_3$-NH ← Gly	1.5	17
OP 7	H-Glu-Gly-Leu-Abu-**p**Tyr-Nle-Asp-Leu-NH_2 $(CH_2)_4$-NH ← Gly	4.0	18
OP 8	H-Glu-Gly-Leu-Abu-**p**Tyr-Nle-Asp-Leu-NH_2 $(CH_2)_5$-NH ← Gly	6.0	19
OP 10	H-Glu-Gly-Leu-Abu-**p**Tyr-Nle-Asp-Leu-NH_2 Gly CH_2-C_6H_{10}-CH_2-NH	14.0	20

Activity: Quotient formed from found activity and basal activity of actually used amount and preparation of SHP-1

is apparently provided. In this case the linker has the additional benefit of a still restricted conformational space which in turn results in enhanced binding affinity and stronger activation. It is important to note that additional effects of the linker due to direct interactions, e.g. by hydrophobic interactions, with the SH2-domain cannot be excluded.

Conclusions

Signal transduction therapy requires selective ligands for protein domains or selective enzyme inhibitors, which are stabilized against enzymatic degradation (proteases, phosphatases) and which can be internalized into living cells. As the protein tyrosine phosphatase SHP-1 plays an important role in the processing of immune cells and in cancerogenesis, intensive studies over the last two decades have addressed the molecular mechanisms of expression, substrate specifity and activity regulation. For this purpose, many peptide ligands for the SH2-domains and substrates have been synthesized and tested. Stabilization of bioactive conformation and stabilization against proteolytic degradation can both be achieved by cylization of the peptide ligands. Our modelled sequence for ligands of the N-terminal SH2-domain contains a backbone-to-side chain cyclization, starting at N-functionalized phosphotyrosine. The syntheses of these cyclic compounds were efficiently achieved by the use of *N*-alkylated dipeptide building blocks, followed by on-resin cyclization and phosphorylation. The potency of stimulating the phosphatase SHP-1 activity was found to significantly depend on ring size, flexibility and hydrophobicity of the lactam bridges. Nevertheless, the results of this study strongly support the use of such cyclic structures for further optimization attempts particularly also in view of the marked resistance to proteolytic degradation imparted by the backbone-to-side chain cyclization.

Acknowledgements

Financial support by the Deutsche Forschungsgemeinschaft (Re 853/10-1) is gratefully acknowledged. We thank Dr Andrea Perner for performing ESI-MS analyses and Dr Wolfgang Guenther for measurement of ^{1}H- and ^{13}C-NMR spectra, Franziska Mussbach and Manuela Flad for estimation of biological activity.

Supporting information

Supporting information may be found in the online version of this article.

References

1 Zoda MS, Reissmann S. Backbone cyclization of peptides via N-functionalized phosphorylated tyrosine. In *Peptides 2008*, Lankinen H, Naervaenen A (eds). FIPS: Helsinki, 2009; 138–139.
2 Zhang J, Somani AK, Siminovitch KA. Roles of SHP-1 tyrosine phosphatase in the negative regulation of cell signalling. *Immunology* 2000; **12**: 361–378.
3 Keilhack H, Müller M, Böhmer S-A, Frank C, Weidner KM, Birchmeier W, Ligensa T, Berndt A, Kosmehl H, Günther B, Müller T, Birchmeier C, Böhmer FD. Negative regulation of Ros receptor tyrosine kinase signaling. An epithelial function of the SH2 domain protein tyrosine phosphatase SHP-1. *J. Cell Biol.* 2001; **152**: 325–334.
4 Li L, Dixon JE. Form, function, and regulation of protein tyrosine phosphatases and their involvement in human diseases. *Semin. Immunol.* 2000; **12**: 75–84.
5 Seo D-W, Li H, Qu CK, Oh J, Kim JS, Diaz T, Wei B, Han JW, Stetler-Stevenson WG. Shp-1 mediates the antiproliferative activity of tissue inhibitor of metalloproteinase-2 in human microvascular endothelial cells. *J. Biol. Chem.* 2006; **281**: 3711–3721.
6 Wu C, Guan Q, Wang Y, Zhao ZJ, Zhou GW. SHP-1 suppresses cancer cell growth by promoting degradation of JAK kinases. *J. Cell Biochem.* 2003; **90**: 1026–1037.
7 Kamata T, Yamashita M, Kimura M, Murata K, Inami M, Shimizu C, Sugaya K, Wang CR, Taniguchi M, Nakayama T. Src-homology 2 domain–containing tyrosine phosphatase SHP-1 controls the development of allergic airway inflammation. *J. Clin. Invest.* 2003; **111**: 109–119.
8 Gavrieli M, Murphy KM. Association of Grb-2 and PI3K p85 with phosphotyrosyl peptides derived from BTLA. *Biochem. Biophys. Res. Com.* 2006; **345**: 1440–1445.
9 Chemnitz JM, Lanfranco AR, Braunstein I, Riley JL. B and T lymphocytes attenuator-mediated signal transduction provides a potent inhibitory signal to primary human CD4 T cells that can be

initiated by multiple phosphotyrosine motifs. *J. Immunol.* 2006; **176**: 6603–6614.
10 Pathak MK, Yi T. Sodium stibogluconate is a potent inhibitor of protein tyrosine phosphatases and augments cytokine responses in hemopoietic cell lines. *J. Immunol.* 2001; **167**: 3391–3397.
11 Yang J, Liang X, Niu T, Meng W, Zhao Z, Zhou GW. Crystal structure of the catalytic domain of protein-tyrosine phosphatase SHP-1. *J. Biol. Chem.* 1998; **273**: 28199–281207.
12 Yang J, Chen Z, Niu T, Liang X, Zhao ZJ, Zhou GW. Structural basis for substrate specificity of protein-tyrosine phosphatase SHP-1. *J. Biol. Chem.* 2000; **275**: 4066–4071.
13 Frank C, Burkhardt C, Imhof D, Ringel J, Zschörnig O, Wieligmann K, Zacharias M, Böhmer F. Effective dephosphorylation of src substrates by SHP-1. *J. Biol. Chem.* 2004; **279**: 11375–11383.
14 Massa PT, Saha S, Wu C, Jarosinski KW. Expression and function of the protein tyrosine phosphatase SHP-1 in oligodendrocytes. *Glia* 2000; **29**: 376–385.
15 Abu-Dayyeh I, Shio MT, Sato S, Akira S, Cousineau R, Oliver M. *Leishmania*-induced IRAK-1 inactivation is mediated by SHP-1 interacting with an evolutionarily conserved KTIM motif. *PLoS Negl. Trop. Dis.* 2008; **2**: e305 (www.plosntd.org).
16 Nadan D, Reiner NE. *Leishmania donovani* engages in regulatory interference by targeting macrophage protein tyrosine phosphatase SHP-1. *Clin. Immunol.* 2005; **114**: 266–277.
17 Imhof D, Wavreille AS, May A, Zacharias M, Tridandapani S, Pei D. Sequence specificity of SHP-1 and SHP-2 Src homology 2 domains. Critical roles of residues beyond the pY+3 Position. *J. Biol. Chem.* 2006; **281**: 20271–20282.
18 Sweeney MC, Wavreille A-S, Park J, Butchar JP, Tridandapani S, Pei D. Decoding protein–protein interactions through combinatorial chemistry: sequence specificity of SHP-1, SHP-2, and SHIP SH2 domains. *Biochemistry* 2005; **44**: 14932–14947.
19 Daeron M, Jaeger SD, Pasquier L, Vivier E. Immunoreceptor tyrosine-based inhibition motifs: a quest in the past and future. *Immunol. Rev.* 2008; **224**: 11–43.
20 Beebe KD, Wang P, Arabaci G, Pei D. Determination of the binding specifity of the SH2 domains of protein tyrosine phosphatase SHP-1 through the screening of a combinatorial phosphotyrosyl peptide library. *Biochemistry* 2000; **39**: 13251–13260.
21 Imhof D, Wieligmann K, Hampel K, Nothmann D, Zoda MS, Schmidt-Arras D, Böhmer F, Reissmann S. Design and biological evaluation of linear and cyclic phosphopeptide ligands of the N-terminal SH2 domain of protein tyrosine phosphatase SHP-1. *J. Med. Chem.* 2005; **48**: 1528–1539.
22 Wieligmann K, Castro LF, Zacharias M. Molecular dynamics simulations on the free and complexed N-terminal SH2 domain of SHP-2. *In Silico Biol.* 2002; **2**: 305–311.
23 Mueller B, Besser D, Kleinwaechter P, Arad O, Reissmann S. Synthesis of N-carboxyalkyl and *N*-aminoalkyl functionalized dipeptide building units for the assembly of backbone cyclic peptides. *J. Pept. Res.* 1999; **54**: 383–393.
24 Besser D, Mueller B, Agricola I, Reissmann S. Synthesis of differentially protected N-acylated reduced pseudodipeptides as building units for backbone cyclic peptides. *J. Pept. Sci.* 2000; **6**: 130–138.
25 Schumann C, Seyfarth L, Greiner G, Reissmann S. Synthesis of different types of dipeptide building units containing N- or C-terminal arginine for the assembly of backbone cyclic peptides. *J. Pept. Res.* 2000; **55**: 428–435.
26 Schumann C, Seyfarth L, Greiner G, Paegelow I, Reissmann S. Synthesis and biological activities of new side chain and backbone cyclic bradykinin analogues. *J. Pept. Res.* 2002; **60**: 128–140.
27 Reissmann S, Imhof D. Development of conformationally restricted analogues of bradykinin and somatostatin using constrained amino acids and different types of cyclization. *Curr. Med. Chem.* 2004; **11**: 2823–2844.
28 Besser D, Müller B, Kleiwächter P, Greiner G, Seyfarth L, Steinmetzer T, Arad O, Reissmann S. Synthesis and characterization of octapeptide somatostatin analogues with backbone cyclization: comparison of different strategies, biological activities and enzymatic stabilities. *J. Prakt. Chem.* 2000; **342**: 537–545.
29 Clark TD, Sastry M, Brown C, Wagner G. Solid-phase synthesis of backbone-cyclized β-helical peptides. *Tetrahedron* 2006; **62**: 9533–9540.
30 Hariton-Gazal E, Rosenbluh J, Zakai N, Fridkin G, Brack-Werner R, Wolff H, Devaux C, Gilon C, Loyter A. Functional analysis of backbone cyclic peptides bearing the arm domain of the HIV Rev protein: characterization of the karyophilic properties and inhibition of Rev-induced gene expression. *Biochemistry* 2005; **44**: 11555–11566.
31 Qvit N, Hatzubai A, Shalev DE, Friedler A, Ben-Neriah Y, Gilon C. Design and synthesis of backbone cyclic phosphorylated peptides: the IκB model. *Biopolymers (Peptide Science)* 2008; **91**: 157–168.
32 Hess S, Linde Y, Ovadia O, Safrai E, Shalev DE, Swed A, Halbfinger E, Lapidot T, Winkler I, Gabinet Y, Feier A, Yarden D, Xiang Z, Portillo FP, Haskell-Luevano C, Gilon C, Hoffmann A. Backbone cyclic peptidomimetic melanocortin-4 receptor agonist as a novel orally administrated drug lead for treating obesity. *J. Med. Chem.* 2008; **51**: 1026–1034.
33 Bitan G, Muller D, Kasher R, Gluhov EV, Gilon C. Building units for N-backbone cyclic peptides. Part 4. Synthesis of protected Nα-functionalized alkyl amino acids by reductive alkylation of natural amino acids. *J. Chem. Soc., Perkin Transactions 1: Organic and Bioorganic Chem.* 1997; **10**: 1501–1510.
34 Gazal S, Gellerman G, Gilon C. Novel Gly building units for backbone cyclization: synthesis and incorporation into model peptides. *Peptides* 2003; **24**: 1847–1852.
35 Loffet A, Zhang HX. Allyl based groups for side chain protection of amino acids. *Int. J. Pept. Prot. Res.* 1993; **42**: 346–351.
36 Guibe F. Allylic protecting groups and their use in a complex environment part ii: allylic protecting groups and their removal through catalytic palladium π-allyl methodology. *Tetrahedron* 1998; **54**: 2967–3042.
37 Nahm S, Weinreb S. *N*-Methoxy-*N*-methylamides as effective acylating agents. *Tetrahedron Lett.* 1981; **22**: 3815–3818.
38 Fehrentz J-A, Castro B. An efficient synthesis of optically active α-(t-butoxycarbonyl-amino)-aldehydes from α-amino acids. *Synthesis* 1983; 676–678.
39 Imhof D, Nothmann D, Zoda MS, Hampel K, Wegert J, Böhmer FD, Reissmann S. Synthesis of linear and cyclic phosphopeptides as ligands for the N-terminal SH_2–domain of protein tyrosine phosphatase SHP-1. *J. Pept. Sci.* 2005; **11**: 390–400.
40 Gothe R, Seyfahrth L, Schumann C, Agricola I, Reissmann S, Lifferth A, Birr C, Filatova MP, Kritsky A, Kibirev V. Combination of allyl protection and Hycram™-linker technology for the synthesis of peptides with problematical amino acids and sequences. *J. Prakt. Chem.* 1999; **341**: 369–377.
41 Perich JW. Synthesis of Tyr(*P*)-containing peptides via "on-line" phosphorylation of the tyrosine residue on the solid phase. *Lett. Pept. Sci.* 1996; **3**: 127–132.
42 Perich JW. Synthesis of phosphopeptides via global phosphorylation on the solid phase: resolution of H-phosphonate formation. *Lett. Pept. Sci.* 1998; **5**: 49–55.
43 Attard TJ, O'Brien-Simpson N, Reynolds EC. Synthesis of phosphopeptides in the Fmoc mode. *Int. J. Pept. Res. Ther.* 2007; **13**: 447–468.
44 Yu HM, Chen ST, Wang KT. Enhanced coupling efficiency in solid-phase peptide synthesis by microwave irradiation. *J. Org. Chem.* 1992; **57**: 4781–4784.
45 Brandt M, Gammeltoft S, Jensen KJ. Microwave heating for solid-phase peptide synthesis: general evaluation and application to 15-mer phosphopeptides. *Inter. J. Pept. Res. and Ther.* 2006; **12**: 349–357.
46 Paul R. *O*-Acylation of tyrosine during peptide synthesis. *J. Org. Chem.* 1963; **28**: 236–237.
47 Girin SK, Svachkin YuP. Natural peptides and their analogs. XV. Study of the effect of a solvent on the rates of *O*- and *N*-acylation under peptide synthesis conditions using the method of p-nitrophenylesters. *Zh. Obshch. Khim.* 1978; **48**: 1887–1891.
48 Martinez J, Tolle JC, Bodanszky M. Side reactions in peptide synthesis: X. Prevention of *O*-acylation during coupling with active esters. *Int. J. Pept. Prot. Res.* 1969; **13**: 22–27.

